

Electroweak form factors of large nuclei as BPS skyrmions

Alberte Xosé López Freire,^{1, 2, *} Christoph Adam,^{1, 2, †} Alberto García Martín-Caro,^{3, 4, ‡} and Diego González Díaz^{1, §}

¹Departamento de Física de Partículas, Universidad de Santiago de Compostela E-15782 Santiago de Compostela, Spain

²Instituto Galego de Física de Altas Enerxías (IGFAE) E-15782 Santiago de Compostela, Spain

³EHU Quantum Center and Department of Physics,

University of the Basque Country UPV/EHU, Bilbao, Spain

⁴Instituto de Física e Ciencias Aeroespaciais (IFCAE), Universidade de Vigo. 32004 Ourense, Spain

(Date: October 31, 2025)

We employ the Bogomolnyi-Prasad-Sommerfield (BPS) Skyrme model within the framework of semi-classical quantization to compute both electromagnetic and neutral current form factors for heavy nuclei. Our results show excellent agreement with the experimental data for low- to moderate momentum transfer. Further, we present an analytic expression of the neutral current form factor for generic nuclei, expressed as a power series in the momentum transfer. Our method provides an alternative to existing phenomenological approaches, and is particularly relevant for precision neutrino experiments where control over model-dependent systematics is essential for probing physics beyond the Standard Model.

Introduction. While the electromagnetic charge distribution of atomic nuclei has been extensively studied through elastic electron scattering experiments, determining the neutron density distribution remains a significant challenge. Enhanced measurements of neutron densities would have profound implications for the equation of state of neutron-rich matter, which is crucial for understanding the structure and evolution of neutron stars [1, 2], as well as for deriving constraints of new physics beyond the Standard Model [3, 4]. Although precise experimental data exist for observables sensitive to neutron distributions—such as nuclear dipole polarizability [5, 6]—hadronic probes introduce model-dependent uncertainties that require careful analysis (see, e.g., Ref. [1]).

In contrast, electroweak processes such as parity-violating electron scattering (PVES) [7, 8] and coherent elastic neutrino-nucleus scattering (CE ν NS) [9] have long been regarded as cleaner and more direct methods for probing neutron densities [10, 11]. Despite their experimental complexity, both techniques have seen significant advances in recent years [12–17]. These efforts provide valuable insights into nuclear structure by enabling the determination of the weak form factor¹, which directly constrains the neutron density distribution within nuclei [18, 19].

Since no precision measurements of neutron density distributions of nuclei are available at the moment, the weak nuclear form factor has to be modelled in order to evaluate experimental cross sections and event rates. Traditionally, the weak form factor has been modelled using phenomenological approaches based on empirical fits to elastic electron scattering data, such as the Klein–Nystrand (KN)

form factor [20] or the Helm form factor [21], both widely used in the CE ν NS community [22]. However, in recent years a theoretical effort has been made to develop actual nuclear structure calculations of ground states and density distributions through microscopic nuclear physics approaches such as density functional theory [23], relativistic mean field methods [24], coupled-cluster theory from first principles [25], shell-model calculations [26], Hartree–Fock plus Bardeen–Cooper–Schrieffer model [27] as well as effective field theory approaches [28, 29], that provide a more accurate description of the weak form factor. However, these highly sophisticated methods often require long computations to determine the properties of individual nuclei or the fitting of a large number of free parameters that reduce their predictive power.

In this work, we present the derivation of electroweak form factors from a very simple effective model of low energy nuclear physics, a variation of the well known Skyrme model [30, 31].

The Skyrme model is a nonlinear field theory of pions which describes nucleons, nuclei, and nuclear matter in terms of appropriately quantized topological soliton solutions (“skyrmions”) [32–35]. Chiral symmetry is realized non-linearly in this model, by pion fields taking values in the group manifold SU(2). A general Skyrme field can be expressed as

$$U(x) = \sigma(x) \mathbb{1} + i\boldsymbol{\pi}(x) \cdot \boldsymbol{\tau}, \quad (1)$$

where $x = (\mathbf{x}, t)$, $\boldsymbol{\tau}$ is the vector of Pauli matrices, $\boldsymbol{\pi} = (\pi_1, \pi_2, \pi_3)$, $\pi_i \in \mathbb{R}$ are the pion fields and $\sigma(x) \in \mathbb{R}$ is an auxiliary field obeying $\sigma^2 + \boldsymbol{\pi} \cdot \boldsymbol{\pi} = 1$. The nontrivial topology of the field space endows each finite energy field configuration U —and, in particular, each skyrmion—with an invariant, integer topological degree,

$$B = \int \mathcal{B}^0 d^3x; \quad \mathcal{B}^\mu = \frac{1}{24\pi^2} \varepsilon^{\mu\nu\rho\sigma} \int \text{Tr}(L_\nu L_\rho L_\sigma) \quad (2)$$

($L_\mu = U^{-1} \partial_\mu U$), which is identified with the baryon number.

* albertexose.lopez.freire@usc.es

† christoph.adam@usc.es

‡ alberto.garcia.martin-caro@uvigo.es

§ diego.gonzalez.diaz@usc.es

¹ In the case of neutrino probes, this is true at least at low momentum transfers where the process remains coherent.

The model originally introduced by Skyrme is defined by the Lagrangian density²

$$\mathcal{L}_S = \mathcal{L}_2 + \mathcal{L}_4 \equiv -\frac{f_\pi^2}{16} \text{Tr}(L_\mu L^\mu) + \frac{1}{32e^2} \text{Tr}([L_\mu, L_\nu]^2) \quad (3)$$

where the quadratic term is dictated by current algebra arguments, and Skyrme introduced the quartic term in order to bypass the scaling instability of \mathcal{L}_2 [36] such that solitonic solutions can exist.

Our starting point is the generalized Skyrme model (first considered in [37]),

$$\mathcal{L}_{GSM} = \mathcal{L}_S + \mathcal{L}_{BPS}, \quad \mathcal{L}_{BPS} \equiv \mathcal{L}_0 + \mathcal{L}_6 \quad (4)$$

where

$$\mathcal{L}_0 \equiv -\mu^2 V(\text{Tr } U) \quad (5)$$

is a potential term which explicitly breaks chiral symmetry down to isospin symmetry and serves, e.g., to give a mass to the pion field. Finally,

$$\mathcal{L}_6 \equiv -\lambda^2 \pi^4 \mathcal{B}_\mu^2, \quad (6)$$

is proportional to the square of the baryon current. This is the only further Poincare-invariant term not more than quadratic in time derivatives that can be added to the model.

Conceptually, the model \mathcal{L}_{GSM} constitutes a candidate theory for nuclear and hadron physics in terms of pions, where baryons and nuclei are realized as topological solitons. However, as an all-encompassing model of nuclei, right now the model lacks precision and is not competitive with the standard methods of nuclear physics.³ On the other hand, the Skyrme model performs much better once more specific problems are considered. It allows, e.g., to predict the rotational excitations of the ground and Hoyle states of ^{12}C [41] or a plethora of several dozens of excitations of ^{16}O [42] with surprising precision. It also provides a good description for high density nuclear matter [43] and, as a consequence, for the inner core of neutron stars [44]. In the high-density regime, the sixth order term (6), which can be related to the omega meson repulsion, is vital for a correct description of nuclear matter [45].

This last observation motivates the introduction [46] and the study [47] of the BPS submodel $\mathcal{L}_{BPS} = \mathcal{L}_0 + \mathcal{L}_6$. The addition of \mathcal{L}_0 is required to avoid the scaling instability. This submodel, which describes a perfect fluid, is a drastic simplification that eliminates, e.g., propagating pion d.o.f. Nevertheless, it reproduces certain bulk properties of large nuclei and nuclear matter surprisingly well.

² The index i in \mathcal{L}_i denotes the power of first derivatives of this term.

³ But there are strong indications that the inclusion of further vector mesons into the model significantly improves its ability to precisely describe nuclear matter [38–40].

Like \mathcal{L}_S [48] and \mathcal{L}_{GSM} [49], the static energy of \mathcal{L}_{BPS} has a topological lower energy bound [46]. Unlike the first two models, the BPS submodel supports infinitely many static BPS solutions that saturate the bound. As a consequence, classical soliton solutions imply zero binding energies for the nuclei they describe, and small, realistic binding energies of large nuclei are achieved by small quantum and Coulomb corrections [50].

Skyrme models also provide a natural arena for the calculation of local charge densities and their associated nuclear form factors, both in the electroweak [51–54], and, more recently, the gravitational [55–57] case. The semi-classical nature of nuclei in such models allows for a simple calculation of current density operators and their expectation values for general nuclei, and the form factors are then found by a simple Fourier transform. We will find that both electromagnetic and weak neutral form factors for large nuclei can be calculated semi-analytically in the BPS Skyrme model, leading to stunning agreement with experimental data.

The BPS Skyrme Model. The static energy of the BPS submodel,

$$\begin{aligned} E_{BPS} &= \int (\lambda^2 \pi^2 \mathcal{B}_0^2 + \mu^2 V(\xi)) d^3x \\ &= \int (\lambda \pi \mathcal{B}_0 \mp \mu \sqrt{V})^2 d^3x \pm 2\pi^2 \mu \lambda |B| \langle \sqrt{V} \rangle \end{aligned} \quad (7)$$

(where $\langle \sqrt{V} \rangle$ is the field space average of \sqrt{V}), can be expressed as the sum of a non-negative term plus a topological lower bound, as is common for BPS theories. Solutions that saturate the bound must obey the simpler first-order BPS equation $\lambda \pi \mathcal{B}_0 = \pm \mu \sqrt{V}$. Further, this equation is compatible with an axially symmetric ansatz leading to spherically symmetric energy and baryon densities. Indeed, introducing $\sigma = \cos \xi$, $\boldsymbol{\pi} = \sin \xi \mathbf{n}$, where \mathbf{n} is a three-component unit vector, and inserting the ansatz $\xi = \xi(r)$ and

$$\mathbf{n}(\theta, \phi) = (\cos(B\phi) \sin \theta, \sin(B\phi) \sin \theta, \cos \theta) \quad (8)$$

in spherical polar coordinates in the BPS equation, results in a first-order ODE for $\xi(r)$. For simple potentials like the pion mass potential $V(\xi) = 1 - \cos \xi$ (to which we will restrict our investigations for simplicity), this equation can be integrated and leads to an exact solution:

$$\xi(r) = 2 \arccos\left(\frac{r}{R_B}\right) \text{ for } r \in [0, R_B], \quad \xi(r) = 0 \text{ otherwise,} \quad (9)$$

with $R_B = \sqrt{2} \sqrt[3]{\frac{B\lambda}{\mu}}$. Hence, the solution is of compacton type, with R_B the compacton radius. Further, the BPS energy is linear in B , and the (compacton, RMS, etc.) radii behave like $R \sim B^{1/3}$, which is a reasonable order zero approximation to physical nuclei. As said, realistic binding energies are provided by small (quantum and Coulomb) corrections.

EW conserved currents and form factors. A simple way to identify the electroweak (EW) currents in the Skyrme model is *i*), to introduce a covariant derivative D_μ into its Lagrangian density which ensures local $SU(2)_L \times U(1)_Y$ invariance [52],

$$D_\mu U = \partial_\mu U + \frac{ie}{2 \sin \theta_W} W_\mu^a \tau_a U - \frac{ie}{2 \cos \theta_W} Y_\mu U \tau_3, \quad (10)$$

and, *ii*), to decompose the gauge fields W_μ^a and Y_μ into the physical vector bosons

$$\begin{aligned} W_\mu^1 &= \frac{1}{\sqrt{2}} (W_\mu^+ + W_\mu^-), & W_\mu^2 &= \frac{i}{\sqrt{2}} (W_\mu^+ - W_\mu^-), \\ W_\mu^3 &= c_W Z_\mu + s_W A_\mu, & Y_\mu &= -s_W Z_\mu + c_W A_\mu, \end{aligned} \quad (11)$$

where $c_W \equiv \cos \theta_W$, $s_W \equiv \sin \theta_W$ and θ_W is the Weinberg angle, with $s_W^2 = 0.223$ [58]. The electroweak currents are now given by the terms that couple to each bosonic field. At this stage, it is convenient to recast these expressions in a more compact form, in terms of the vector and axial-vector currents. The derivative terms in the general Skyrme model are invariant separately under left ($U \rightarrow VU$) and right ($U \rightarrow UW$) chiral transformations. It is useful to rewrite them in terms of the vector and axial-vector transformations

$$\begin{aligned} V : \quad U &\rightarrow W^\dagger UW, \quad W \in SU(2) \\ A : \quad U &\rightarrow WUW. \end{aligned} \quad (12)$$

In the BPS Skyrme model, their associated Noether current densities are

$$J_{k,V(A)}^\alpha = \mp \frac{\lambda^2 \pi^2}{4} \epsilon^{\alpha\nu\rho\sigma} \mathcal{B}_\nu \text{Tr}\{T_k^\mp L_\rho L_\sigma\} \quad (13)$$

where $T_k^\mp \equiv iU^\dagger [\frac{\tau_k}{2}, U]_\mp$ and $[\cdot, \cdot]_\mp$ are commutator and anti-commutator, respectively. The weak neutral current is then ($g \sin \theta_W = e$)

$$J_{NC}^\nu = -\frac{g}{c_W} \left[\frac{1}{2} (J_{3,V}^\nu - J_{3,A}^\nu) - s_W^2 J_{EM}^\nu \right]. \quad (14)$$

For the electromagnetic current, only the vector current contribution can be derived in this way. An additional baryon current density component originates from the Wess-Zumino-Witten term [59], which is induced by QCD anomalies and must be incorporated into the model. However, for our purposes, it is sufficient to use the Gell-Mann-Nishijima formula, leading to

$$J_{EM}^\nu = J_{3,V}^\nu + \frac{1}{2} \mathcal{B}^\nu. \quad (15)$$

Semi-classical quantization. The classical skyrmion solutions only provide the mass and atomic weight number (=baryon number) for the nucleus they are supposed to describe. For a description of the spin and the number of protons Z and neutrons N , which are good quantum numbers of nuclei, the corresponding rotational and isorotational degrees of freedom must be introduced and quantized. Here, isospin is related to Z and N via $2i_3 = Z - N$,

where \hat{I}_3 is the third component of the isospin operator, and i_3 its eigenvalue for a nuclear state.

In the Skyrme model this is achieved by a well-known procedure called rigid rotor quantization. In a first step, time-dependent rotations and isorotations are introduced into a static skyrmion $U_0(\mathbf{x})$ via $U(t, \mathbf{x}) = A(t)U_0(R(t)\mathbf{x})A^\dagger(t)$, where $A(t) \in SU(2)$ and $R(t) \in SO(3)$. When this expression is inserted into the Lagrangian, the terms without time derivatives just add up to minus the skyrmion mass, because the (iso)rotations are symmetries. The time-derivative terms, on the other hand, lead to a quadratic form in angular velocities. In a next step, this rigid rotor Lagrangian is transformed to an equivalent Hamiltonian by a Legendre transformation, and the angular velocities are replaced by their conjugate momenta, the body-fixed spin (\mathbf{L}) and isospin (\mathbf{K}) angular momenta. In addition to introducing the rotational d.o.f., the matrix R and its iso-rotational equivalent $(R_A)_{ij} = \frac{1}{2} \text{Tr}(\tau_i A \tau_j A^\dagger)$ play a second role by providing the transformations from the body-fixed to the space-fixed spin (\mathbf{J}) and isospin (\mathbf{I}) angular momenta via $\mathbf{I} = -R_A \mathbf{K}$ and $\mathbf{J} = -R^T \mathbf{L}$, which implies $\mathbf{I}^2 = \mathbf{K}^2$ and $\mathbf{J}^2 = \mathbf{L}^2$.

The angular momenta $\mathbf{I}, \mathbf{J}, \mathbf{K}, \mathbf{L}$ are promoted to quantum operators $\hat{\mathbf{I}}$, etc., by imposing the usual angular momentum commutation relations. Nuclear states in this space are characterized by the corresponding eigenvalues, $|\Psi\rangle = |ii_3k_3\rangle \otimes |jj_3l_3\rangle$. The currents discussed above and their time components, which are the relevant ones for the form factors, become non-trivial operators if they contain time derivatives of the Skyrme field. This is not the case for the baryon current, which acts trivially (proportional to the identity) in this space. The components $J_{k,V(A)}^0$, on the other hand, are linear in time derivatives and therefore become linear operators in $\hat{\mathbf{I}}$, etc.

For the BPS Skyrme model and for the axially symmetric ansatz (8), the vector current operator $J_{3,V}^0$ and its expectation value w.r.t. $|\Psi\rangle$ have already been calculated in [50], see eq. (18) of that paper (a much more detailed calculation can be found in [60]). The result is

$$\begin{aligned} \langle \hat{J}_{3,V}^0 \rangle &= 4\pi^4 \frac{\lambda^2 i_3}{\mathcal{I}_3} r^2 (\mathcal{B}^0(r))^2 \frac{1 + B^{-2} \cos^2 \theta}{3B^2 + 1} \\ &= \frac{\lambda^2 i_3}{\mathcal{I}_3 r^2} \xi_r^2 \sin^4 \xi \frac{B^2 + \cos^2 \theta}{3B^2 + 1}. \end{aligned} \quad (16)$$

This is approximately spherically symmetric for sufficiently large B , where $\frac{B^2 + \cos^2 \theta}{3B^2 + 1} \sim \frac{1}{3}$. Further, \mathcal{I}_3 is the 3-3 component of the isospin moment-of-inertia tensor, which is the integral of a known expression of ξ (given in (9)) and its derivative ξ_r . For our choice of potential, the integral is analytic and given by:

$$\mathcal{I}_3 = \frac{64\pi \mu^2}{105 B^2} R_B^5. \quad (17)$$

In principle, we are still missing the expectation value of the axial-vector current operator. However, it turns out that, for the axially symmetric ansatz, $\langle \hat{J}_{3,A}^0 \rangle = 0$.

This result agrees with the fact that the axial-vector contribution vanishes for $0^+ \rightarrow 0^+$ transitions [61].

Thus, for the charge densities of our interest, we get

$$\langle \hat{J}_{\text{EM}}^0 \rangle = \frac{1}{2} \mathcal{B}_0 + \langle \hat{J}_{3,V}^0 \rangle, \quad (18)$$

and

$$\langle \hat{J}_{\text{NC}}^0 \rangle = \frac{g}{c_W} \left(\frac{1}{2} s_W^2 \mathcal{B}_0 - \left(\frac{1}{2} - s_W^2 \right) \langle \hat{J}_{3,V}^0 \rangle \right). \quad (19)$$

Computing the form factors. Form factors take into account the extended character of nuclei in scattering and other interaction processes. In the Breit frame, where only momentum \mathbf{q} but no energy is transferred from the nucleus to its scattering partner (electron or neutrino), the form factor is the purely spatial Fourier transform of the relevant charge distribution $\mathcal{Q}_\rho \sim \langle \hat{J}_\rho^0 \rangle$ [53]:

$$F_\rho(\mathbf{q}) = \int \frac{\mathcal{Q}_\rho(\mathbf{x})}{Q_\rho} e^{-i\mathbf{q} \cdot \mathbf{x}} d^3\mathbf{x} \approx \int \frac{4\pi \mathcal{Q}_\rho(r) \sin qr}{Q_\rho} \frac{qr}{r^2} dr \quad (20)$$

where ρ above denotes either the electromagnetic (EM) or weak neutral current (NC), respectively. In the last equation, we assume an approximate spherical symmetry of \mathcal{Q}_ρ . Furthermore, the form factor is normalized to $F(q=0) = 1$ by convention, with the normalization factor being the associated total charge, $Q_\rho = 4\pi \int_0^\infty r^2 \mathcal{Q}_\rho(r) dr$.

Since only the small momentum transfer region is experimentally accessible for weak charge form factors, it is convenient to expand the weak form factor about $q=0$ in terms of the even moments of the density distribution,

$$F_\rho(q) = \sum_{n=0}^{\infty} \frac{(-1)^n}{(1+2n)!} \langle R_\rho^{2n} \rangle (B, i_3) q^{2n}, \quad (21)$$

with

$$\langle R_\rho^{2n} \rangle = \frac{4\pi}{Q_\rho} \int r^{2n+2} \rho(r) dr. \quad (22)$$

In the BPS Skyrme model, the density $\langle \hat{J}_{3,V}^0 \rangle$ is proportional to $r^2 (\mathcal{B}^0)^2$, (see (16)), hence we can write the moments of the EW charge densities in terms of the moments of \mathcal{B}^0 and $(\mathcal{B}^0)^2$:

$$\int r^{2n+2} (r \mathcal{B}^0)^2 dr = \frac{4\mu^2}{\pi^4 \lambda^2} \frac{R_B^{2n+5}}{(2n+5)(2n+7)}, \quad (23)$$

$$\int r^{2n+2} \mathcal{B}^0 dr = \frac{\mu}{2\sqrt{2}\lambda\pi^{3/2}} \frac{\Gamma(n+3/2)}{\Gamma(n+3)} R_B^{2n+3}, \quad (24)$$

where Γ represents Euler's gamma function. For instance, the weak neutral current form factor $F_{NC}(q)$ for *any* given nucleus with quantum numbers (B, i_3) leads to the moments

$$\langle R_{\text{NC}}^{2n} \rangle = \frac{4\pi R_B^{2n}}{Q_{\text{NC}}} \left[\frac{s_W^2}{2} \frac{B\Gamma(n+3/2)}{\pi^{3/2}\Gamma(n+3)} + \frac{35(s_W^2 - 1/2)i_3}{4\pi(2n+5)(2n+7)} \right], \quad (25)$$

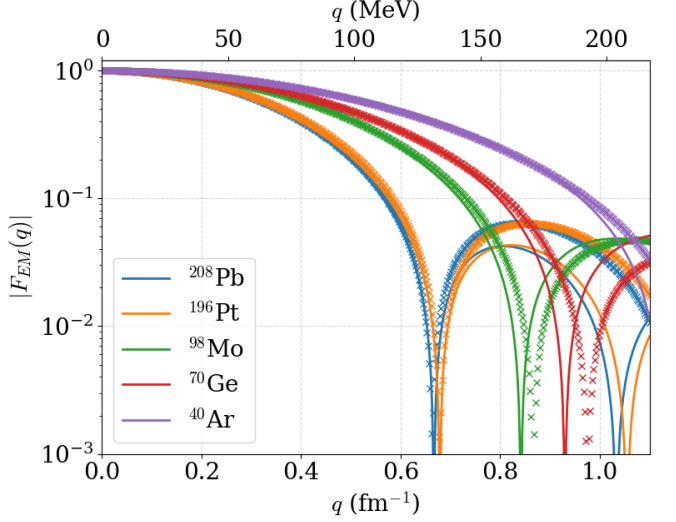


FIG. 1: Electromagnetic form factors for different nuclei. Solid lines represent the prediction of the BPS model, while the crosses correspond to the experimental parametrization of [62].

where $Q_{\text{NC}} = \frac{1}{2} (s_W^2 B - (1 - 2s_W^2) i_3)$. Similarly, for the electromagnetic charge form factor, we get

$$\langle R_{\text{EM}}^{2n} \rangle = \frac{4\pi R_B^{2n}}{Q_{\text{EM}}} \left[\frac{B\Gamma(n+3/2)}{2\pi^{3/2}\Gamma(n+3)} + \frac{35i_3}{4\pi(2n+5)(2n+7)} \right], \quad (26)$$

with $Q_{\text{EM}} = \frac{B}{2} + i_3$. In both types of interaction, the Taylor series approximation shows very good agreement in the region considered, assuming terms up to $n=10$.

Finally, R_B depends on the values for the free parameters λ and μ , which are fitted to nuclear masses and radii (see Sec. A). With our choice of values, we have

$$R_B = 1.3599 B^{1/3} \text{ fm}. \quad (27)$$

We show the resulting electromagnetic form factors for a representative set of medium ($B \simeq 40$) to large ($B \simeq 200$) nuclei in Fig. 1. In Fig. 2, we show the weak neutral form factors for ^{208}Pb and ^{48}Ca , where experimental results are available from recent PVES experiments.

Conclusions. In this work, we have explored the electroweak currents and the corresponding form factors for large-mass nuclei, which are experimentally relevant to the study of coherent elastic neutrino-nucleus scattering (CE ν NS) and parity-violating electron scattering (PVES) experiments, from the point of view of the generalized Skyrme model, in which nuclei are modelled as topological solitons. In this approach, the computation of spatial densities for electroweak charges is reduced to finding the classical soliton configuration.

We restricted our calculation to the Bogomolnyi-Prasad-Sommerfield term under the (simplest) pion mass potential, a sub-model which has shown its prowess in the description of high-density baryonic systems, and

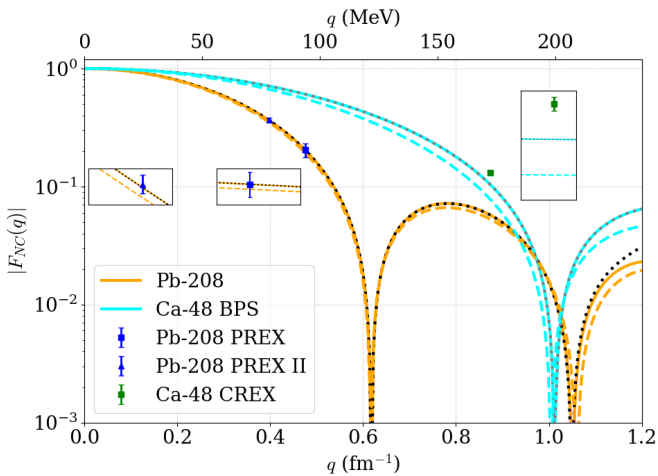


FIG. 2: Neutral current form factors for ^{208}Pb and ^{48}Ca . Solid lines represent the BPS model prediction, while dotted black/grey lines correspond to the Taylor series (21) for ^{208}Pb and ^{48}Ca , respectively, up to $n = 10$. Finally, dashed lines represent the KN model prediction. Experimental results are obtained from [16, 63, 64].

that enables the classical soliton solution to be obtained analytically. The model contains two parameters which combine effectively into a single global one, R_B (root-mean-square charge radius), on which form factors analytically depend. This represents, arguably, the simplest solution of the generalized Skyrme model and,

yet, the calculated electromagnetic form factors display an excellent agreement with the experimental data for momentum transfers of up to $\sim 150\text{MeV}$. For ^{208}Pb and ^{48}Ca , where experimental data for the weak neutral form factor exist, our model better reproduces these results than the widely used Klein-Nystrand (KN) model, despite the fact that in the latter the model parameters are fitted individually for each nucleus. Our work can be interpreted on the one hand as an effective field theory calculation of the electromagnetic and weak form factors of nuclei. On the other hand it offers a simple single-parameter analytical formula for them. As data keeps accumulating on CE ν NS and PVES scattering experiments, a first-principle global description with a minimum of free parameters is called to be a powerful asset to identify trends or anomalies, that could point to Beyond Standard Model physics.

Acknowledgements. The authors acknowledge financial support from the Spanish Research State Agency under project PID2023-152762NB-I00, the Xunta de Galicia under the project ED431F 2023/10 and the CIGUS Network of Research Centres, the María de Maeztu grant CEX2023-001318-M funded by MICIU/AEI /10.13039/501100011033, and the European Union ERDF. The work of A.X.L.F. was also supported by grant ED481A-2025 (Consellería de Cultura, Educación, Formación Profesional y Universidades, Xunta de Galicia). A.G.M.C. is supported by grants No. ED481B-2025/059 and ED431B-2024/42 (Consellería de Cultura, Educación, Formación Profesional y Universidades, Xunta de Galicia).

-
- [1] M. Thiel, C. Sfienti, J. Piekarewicz, C. J. Horowitz, and M. Vanderhaeghen, *J. Phys. G* **46**, 093003 (2019), [arXiv:1904.12269 \[nucl-ex\]](#).
- [2] B. T. Reed, F. J. Fattoyev, C. J. Horowitz, and J. Piekarewicz, *Phys. Rev. Lett.* **126**, 172503 (2021), [arXiv:2101.03193 \[nucl-th\]](#).
- [3] J. Barranco, O. G. Miranda, and T. I. Rashba, *JHEP* **12**, 021 (2005), [arXiv:hep-ph/0508299](#).
- [4] B. Dutta, S. Liao, S. Sinha, and L. E. Strigari, *Phys. Rev. Lett.* **123**, 061801 (2019), [arXiv:1903.10666 \[hep-ph\]](#).
- [5] A. Tamii *et al.*, *Phys. Rev. Lett.* **107**, 062502 (2011), [arXiv:1104.5431 \[nucl-ex\]](#).
- [6] T. Hashimoto *et al.*, *Phys. Rev. C* **92**, 031305 (2015), [arXiv:1503.08321 \[nucl-ex\]](#).
- [7] C. Y. Prescott *et al.*, *Phys. Lett. B* **77**, 347 (1978).
- [8] P. Souder and K. D. Paschke, *Front. Phys. (Beijing)* **11**, 111301 (2016).
- [9] D. Z. Freedman, *Phys. Rev. D* **9**, 1389 (1974).
- [10] E. Ciuffoli, J. Evslin, Q. Fu, and J. Tang, *Phys. Rev. D* **97**, 113003 (2018), [arXiv:1801.02166 \[physics.ins-det\]](#).
- [11] L. A. Russo *et al.*, (2022), 10.1088/1361-6471/adae26, [arXiv:2203.09030 \[hep-ph\]](#).
- [12] D. Akimov *et al.* (COHERENT), *Science* **357**, 1123 (2017), [arXiv:1708.01294 \[nucl-ex\]](#).
- [13] D. Akimov *et al.* (COHERENT), *Phys. Rev. D* **100**, 115020 (2019), [arXiv:1909.05913 \[hep-ex\]](#).
- [14] S. Adamski *et al.* (COHERENT), (2024), [arXiv:2406.13806 \[hep-ex\]](#).
- [15] S. Abrahamyan *et al.*, *Phys. Rev. Lett.* **108**, 112502 (2012), [arXiv:1201.2568 \[nucl-ex\]](#).
- [16] D. Adhikari *et al.* (CREX), *Phys. Rev. Lett.* **129**, 042501 (2022), [arXiv:2205.11593 \[nucl-ex\]](#).
- [17] N. Ackermann *et al.* (CONUS), *Phys. Rev. Lett.* **133**, 251802 (2024).
- [18] M. Cadeddu, F. Dordei, C. Giunti, Y. F. Li, and Y. Y. Zhang, *Phys. Rev. D* **101**, 033004 (2020), [arXiv:1908.06045 \[hep-ph\]](#).
- [19] D. K. Papoulias, T. S. Kosmas, R. Sahu, V. K. B. Kota, and M. Hota, *Phys. Lett. B* **800**, 135133 (2020), [arXiv:1903.03722 \[hep-ph\]](#).
- [20] S. Klein and J. Nystrand, *Phys. Rev. C* **60**, 014903 (1999), [arXiv:hep-ph/9902259](#).
- [21] R. H. Helm, *Phys. Rev.* **104**, 1466 (1956).
- [22] D. Baxter *et al.*, *JHEP* **02**, 123 (2020), [arXiv:1911.00762 \[physics.ins-det\]](#).
- [23] K. Patton, J. Engel, G. C. McLaughlin, and N. Schunck, *Phys. Rev. C* **86**, 024612 (2012), [arXiv:1207.0693 \[nucl-th\]](#).
- [24] J. Yang, J. A. Hernandez, and J. Piekarewicz, *Phys. Rev. C* **100**, 054301 (2019), [arXiv:1908.10939 \[nucl-th\]](#).

- [25] C. G. Payne, S. Bacca, G. Hagen, W. Jiang, and T. Papenbrock, *Phys. Rev. C* **100**, 061304 (2019), arXiv:1908.09739 [nucl-th].
- [26] R. Abdel Khaleq, J. L. Newstead, C. Simenel, and A. E. Stuchbery, *Phys. Rev. D* **111**, 033003 (2025), arXiv:2405.20060 [hep-ph].
- [27] G. Co', M. Anguiano, and A. M. Lallena, *JCAP* **04**, 044 (2020), arXiv:2001.04684 [nucl-th].
- [28] O. Tomalak, P. Machado, V. Pandey, and R. Plestid, *JHEP* **02**, 097 (2021), arXiv:2011.05960 [hep-ph].
- [29] M. Hoferichter, J. Menéndez, and A. Schwenk, *Phys. Rev. D* **102**, 074018 (2020).
- [30] T. Skyrme, *Proc. Roy. Soc. Lond. A* **260**, 127 (1961).
- [31] N. Manton, *Skyrmions – A Theory of Nuclei* (World Scientific, 2022).
- [32] G. S. Adkins, C. R. Nappi, and E. Witten, *Nuclear Physics B* **228**, 552 (1983).
- [33] G. S. Adkins and C. R. Nappi, *Nuclear Physics B* **233**, 109 (1984).
- [34] L. Carson, *Nucl. Phys. A* **535**, 479 (1991).
- [35] R. A. Battye, N. S. Manton, P. M. Sutcliffe, and S. W. Wood, *Physical Review C* **80**, 034323 (2009).
- [36] G. H. Derrick, *J. Math. Phys.* **5**, 1252 (1964).
- [37] A. Jackson, A. D. Jackson, A. S. Goldhaber, G. E. Brown, and L. C. Castillejo, *Phys. Lett. B* **154**, 101 (1985).
- [38] C. Naya and P. Sutcliffe, *Phys. Rev. Lett.* **121**, 232002 (2018).
- [39] D. Harland, P. Leask, and M. Speight, *JHEP* **06**, 116 (2024), arXiv:2404.11287 [hep-th].
- [40] M. Huidobro, P. Leask, C. Naya, and A. Wereszczynski, *JHEP* **01**, 048 (2025), arXiv:2405.20757 [hep-th].
- [41] P. H. C. Lau and N. S. Manton, *Phys. Rev. Lett.* **113**, 232503 (2014).
- [42] C. J. Halcrow, C. King, and N. S. Manton, *Phys. Rev. C* **95**, 031303 (2017).
- [43] C. Adam, A. García Martín-Caro, M. Huidobro, and A. Wereszczynski, *Symmetry* **15**, 899 (2023), arXiv:2305.06639 [nucl-th].
- [44] C. Adam, A. García Martín-Caro, M. Huidobro, R. Vázquez, and A. Wereszczynski, *Phys. Lett. B* **811**, 135928 (2020), arXiv:2006.07983 [hep-th].
- [45] C. Adam, M. Haberichter, and A. Wereszczynski, *Phys. Rev. C* **92**, 055807 (2015), arXiv:1509.04795 [hep-th].
- [46] C. Adam, J. Sanchez-Guillen, and A. Wereszczynski, *Phys. Lett. B* **691**, 105 (2010), arXiv:1001.4544 [hep-th].
- [47] C. Adam, J. Sanchez-Guillen, and A. Wereszczynski, *Phys. Rev. D* **82**, 085015 (2010), arXiv:1007.1567 [hep-th].
- [48] L. D. Faddeev, *Lett. Math. Phys.* **1**, 289 (1976).
- [49] C. Adam and A. Wereszczynski, *Phys. Rev. D* **89**, 065010 (2014), arXiv:1311.2939 [hep-th].
- [50] C. Adam, C. Naya, J. Sanchez-Guillen, and A. Wereszczynski, *Phys. Rev. Lett.* **111**, 232501 (2013), arXiv:1312.2960 [nucl-th].
- [51] E. Braaten and L. Carson, *Phys. Rev. D* **39**, 838 (1989).
- [52] E. Braaten, S.-M. Tse, and C. Willcox, *Phys. Rev. D* **34**, 1482 (1986).
- [53] M. Karliner, C. King, and N. S. Manton, *J. Phys. G* **43**, 055104 (2016), arXiv:1510.00280 [nucl-th].
- [54] A. García Martín-Caro and C. Halcrow, (2023), arXiv:2312.04335 [nucl-th].
- [55] C. Cebulla, K. Goeke, J. Ossmann, and P. Schweitzer, *Nucl. Phys. A* **794**, 87 (2007), arXiv:hep-ph/0703025.
- [56] A. García Martín-Caro, M. Huidobro, and Y. Hatta, *Phys. Rev. D* **108**, 034014 (2023), arXiv:2304.05994 [nucl-th].
- [57] A. García Martín-Caro, M. Huidobro, and Y. Hatta, *Phys. Rev. D* **110**, 034002 (2024), arXiv:2312.12984 [hep-ph].
- [58] P. J. Mohr, D. B. Newell, B. N. Taylor, and E. Tiesinga, *Rev. Mod. Phys.* **97**, 025002 (2025).
- [59] C. G. Callan, Jr. and E. Witten, *Nucl. Phys. B* **239**, 161 (1984).
- [60] C. Naya Rodríguez, Ph.D. thesis, U. Santiago de Compostela (main) (2015).
- [61] Y. Giomataris and J. D. Vergados, *Phys. Lett. B* **634**, 23 (2006), arXiv:hep-ex/0503029.
- [62] H. De Vries, C. W. De Jager, and C. De Vries, *Atom. Data Nucl. Data Tabl.* **36**, 495 (1987).
- [63] C. J. Horowitz *et al.*, *Phys. Rev. C* **85**, 032501 (2012), arXiv:1202.1468 [nucl-ex].
- [64] D. Adhikari *et al.* (PREX), *Phys. Rev. Lett.* **126**, 172502 (2021), arXiv:2102.10767 [nucl-ex].
- [65] IAEA, “International atomic energy agency nuclear data services,” (2025).

Appendix A: Fitting the free parameters

To fix the parameter values of λ and μ from the BPS lagrangian density, we fitted the classical skyrmion energy,

$$E_{BPS} = \frac{64\sqrt{2}\pi}{15} \mu \lambda B, \quad (A1)$$

and the root-mean-square charge radii of the BPS skyrmions,

$$\sqrt{\langle r^2 \rangle} = \sqrt{\frac{\int r^2 \langle J_{EM}^0 \rangle dV}{\int \langle J_{EM}^0 \rangle dV}} = \frac{1}{3} \left(\frac{\lambda}{\mu} \right)^{1/3} \sqrt{\frac{B^{2/3} (20i_3 + 9B)}{(2i_3 + B)}}, \quad (A2)$$

to the masses and charge radii of the nuclei listed in table I, using a least mean squares fit. The values for the parameters after fitting are

$$\begin{aligned} \lambda &= 6.6080 \text{ MeV}^{1/2} \text{fm}^{3/2}, \\ \mu &= 7.4323 \text{ MeV}^{1/2} \text{fm}^{-3/2}, \end{aligned} \quad (A3)$$

leading to eq. (27) and $E_{BPS} = 931.0 B$ MeV. One can straightforwardly see from the mass vs charge radius data plotted in Fig. 3 that the fit is indeed especially accurate for the region of nuclear masses ≥ 50 GeV. This region is precisely the most interesting from the experimental point of view, as the cross section for coherent neutrino-nucleus scattering is enhanced by a large number of neutrons as N^2 .

Nucleus	B	Z	i_3	R (fm)	m (GeV)
^{12}C	12	6	0	2.4702	11.175
^{16}O	16	8	0	2.6991	14.895
^{20}Ne	20	10	0	3.0055	18.618
^{24}Mg	24	12	0	3.0570	22.336
^{40}Ar	40	18	-2	3.4274	37.216
^{48}Ca	48	20	-4	3.4771	44.657
^{76}Ge	76	32	-6	4.0811	70.704
^{86}Sr	86	38	-5	4.2307	80.005
^{116}Sn	116	50	-8	4.6250	107.936
^{124}Sn	124	50	-12	4.6735	115.391
^{130}Xe	130	54	-11	4.7818	120.977
^{136}Ba	136	56	-12	4.8334	126.566
^{188}Os	188	76	-18	5.3993	175.041
^{192}Pt	192	78	-18	5.4169	178.771
^{194}Pt	194	78	-19	5.4236	180.635
^{200}Hg	200	80	-20	5.4551	186.228
^{204}Hg	204	80	-22	5.4744	189.959
^{206}Pb	206	82	-21	5.4902	191.822
^{208}Pb	208	82	-22	5.5012	193.687

TABLE I: Nuclei used to fix the parameters. R is the root-mean-square nuclear charge radius. Data from [65].

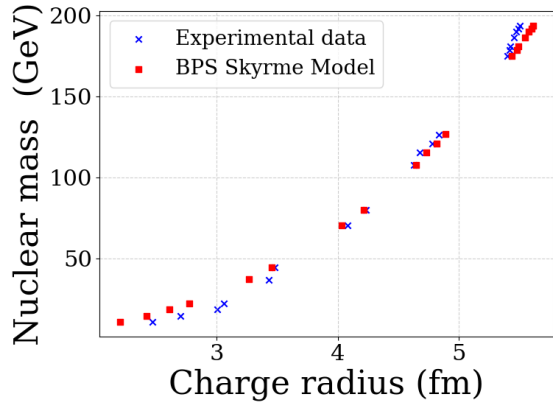


FIG. 3: Nuclear mass and charge radius experimental data of the nuclei used to fit the parameters and their predicted values using the BPS Skyrme model with the fitting of (A3).